Thermal annealing of indium-doped $Cd_{0.7}Hg_{0.3}Te$ epitaxial films

© K.D. Mynbaev[1], N.L. Bazhenov[1], M.V. Dorogov[2], V.S. Balashov[2], V.S. Varavin[3], V.G. Remesnik[3], N.N. Mikhailov[3]

[1] Ioffe Institute,
194021 St. Petersburg, Russia
[2] ITMO University,
197198 St. Petersburg, Russia
[3] Rzhanov Institute of Semiconductor Physics, Siberian Branch, Russian Academy of Sciences,
630090 Novosibirsk, Russia

E-mail: mynkad@mail.ioffe.ru

Received May 5, 2026
Revised June 22, 2026
Accepted June 22, 2026

The optical properties (optical reflection and transmission, as well as photoluminescence) and elemental composition (determined by X-ray energy-dispersive spectroscopy) of indium-doped, thermally annealed epitaxial $Cd_{0.7}Hg_{0.3}Te$ films have been investigated. The results demonstrate a stabilizing effect of indium on the material's properties at 300 K. Annealing of doped $Cd_{0.7}Hg_{0.3}Te$ appeared to be associated with changes in its defect structure that modify its optical properties at low temperatures inversely to those observed in the un-doped material.

Keywords: CdHgTe, doping, annealing, defects, photoluminescence.

DOI: 10.61011/SC.2026.05.63989.9658

$Cd_xHg_{1-x}Te$ (MCT) solid solutions with a CdTe content (composition) $x \approx 0.7$ ($Cd_{0.7}Hg_{0.3}Te$) are in demand for near-infrared photodiodes for astronomical observations [1] and for spacer and barrier layers in laser heterostructures (HSs) [2] and *n*B*n* photodetectors [3]. Indium is commonly introduced to obtain MCT with a specified donor doping level, and successful indium doping has also been demonstrated for $Cd_{0.7}Hg_{0.3}Te$ [4]. Understanding changes in doped MCT during thermal annealing remains important for both compositionally uniform epitaxial films (EFs) and multilayer HSs. Such annealing *de facto* already occurs *in situ* during sequential growth of the HS layers and is also used in post-growth processing. Here we report changes in the properties of indium-doped $Cd_{0.7}Hg_{0.3}Te$ EFs and $Cd_{0.7}Hg_{0.3}Te$/HgTe HSs induced by thermal annealing.

The growth and doping procedures were described in Ref. [4]. The $Cd_{0.7}Hg_{0.3}Te$ layer in the HS was $\sim 3\,\mu$m thick, and the HgTe layer was 200 nm thick. To study the EFs, the HgTe layer was removed from the HS surface in a 0.05 % solution of Br_2 in $(CH_3)_2NC(O)$. The indium concentrations C_{In} specified during growth and the electron concentrations n_{77} in the as-grown EFs, determined by Hall measurements at $T = 77$ K, are listed in Table 1; structures *A* and *A*' were not doped with indium. These structures were annealed ($T = 410\,^\circ$C, 7 min) under mercury-deficient conditions; the other anneals ($T = 225\,^\circ$C, 24 h) were performed in saturated Hg vapor.

The optical properties were investigated by optical reflectance (OR), optical transmittance (OT), and photoluminescence (PL). OR and OT spectra were measured at $T = 293$ K using an InfraLUM-801 Fourier-transform spectrometer with a short-wavelength accessory or a PerkinElmer Lambda 1050 grating spectrometer. PL spectra were recorded at $T = 4.2$ and 293 K using an MDR-23 monochromator, excitation by a semiconductor laser (wavelength $\lambda = 1.03\,\mu$m), and detection with a germanium photodiode and lock-in amplification. The elemental composition of HSs and EFs and its distribution across cleaved cross sections were examined by energy-dispersive X-ray spectroscopy (EDX) using a TESCAN MIRA3 electron microscope. Measurements were performed at an accelerating voltage of 20 kV using GaP standards (for Ga, analytical line $K\alpha_1$), InAs (for As, $L\alpha_1$), Cd (for Cd, $L\alpha_1$), and HgTe (for Hg, $M\alpha_1$, and Te, $L\alpha_1$).

Figure 1, *a* shows the OT spectra of structure *B*. Spectrum *1* of the initial HS has low transmittance and a diffuse edge, owing to the HgTe layer. After this layer was removed, the transmittance increased considerably and the OT edge became sharp (spectrum *2*). Annealing the HS shifted the OT edge slightly toward lower energy (LE) (spectrum *3*); annealing the EF produced only a small change in the OT edge position (spectrum *4*). For undoped EFs, annealing shifted the OT edge toward higher energy (HE); spectra *5* and *6* in Figure 1, *a* show the as-grown and annealed *A*' film, respectively. The same result was reported in Ref. [4] for structure *A*. For structure *D*, annealing shifted the OT edge toward LE in both the HS and EF.

Table 1. Parameters of the structures studied

Structure	Composition x	C_{In}, cm^{-3}	n_{77}, cm^{-3}
A	0.72	0	$1.0 \cdot 10^{14}$
A'	0.70	0	$3.0 \cdot 10^{14}$
B	0.71	$1.1 \cdot 10^{16}$	$1.9 \cdot 10^{16}$
C	0.71	$5.4 \cdot 10^{17}$	$3.7 \cdot 10^{17}$
D	0.72	$4.3 \cdot 10^{18}$	$1.5 \cdot 10^{18}$

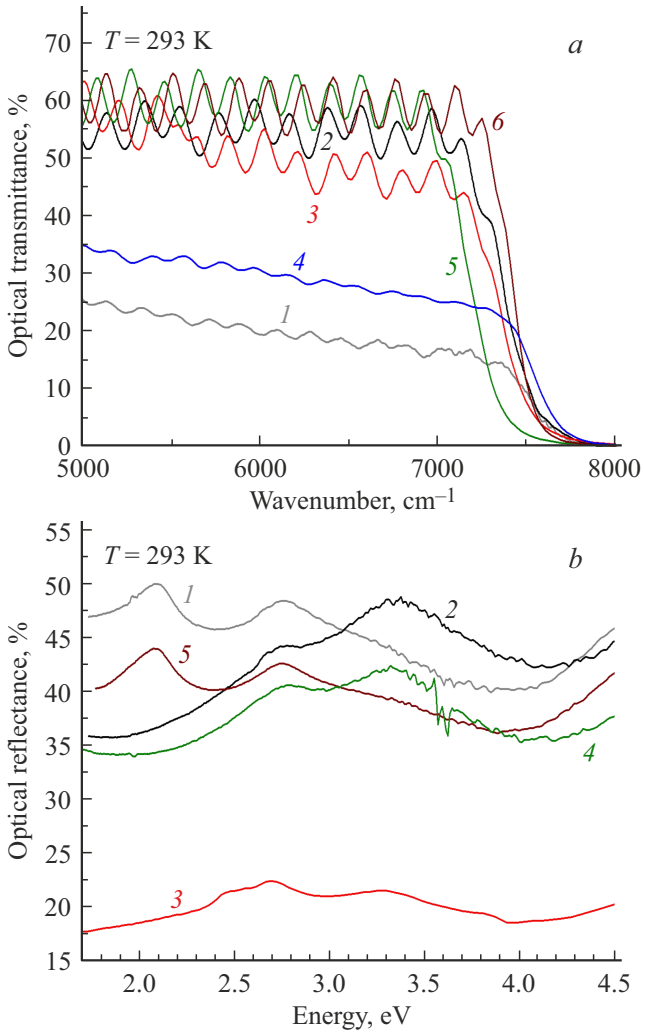


Figure 1. Optical transmittance (*a*) and reflectance (*b*) spectra of structure *B*: *1* — as-grown HS, *2* — as-grown EF, and *3* — annealed HS. Panel *a* also shows the OT spectra of annealed EF *B* (*4*) and as-grown (*5*) and annealed (*6*) EF *A*'. Panel *b* shows the OR spectra of as-grown EF *A*' (*4*) and the HgTe reference sample (*5*).

Figure 1, *b* shows the OR spectra of structure *B*. All contain the characteristic E_1 and $E_1 + \Delta$ peak doublet arising from the $L_{4,5} \rightarrow L_6$ and $L_6 \rightarrow L_6$ optical transitions, respectively [5]. The peak positions in the *B* HS (spectrum *1*) correspond to those of HgTe, whose spectrum *5* is shown for comparison. After the HgTe layer was removed, the peak energies in EF spectrum *2* were close to those of the *A*' EF (spectrum *4*) and corresponded to the specified solid-solution composition. Annealing the HS shifted the OR peaks slightly toward LE (spectrum *3*). The reduction in OT and OR intensity after processing (etching and annealing) resulted from deterioration of the surface quality.

Analysis of the PL spectra showed that the full width at half maximum (FWHM) of the PL bands of all as-grown structures at $T = 4.2$ K was ~ 18 meV. The spectra of EFs *C* and *D* also contained lines due to transitions from the indium level [4]. For structure *A*, annealing either the HS or the EF shifted the $Cd_{0.7}Hg_{0.3}Te$ PL peaks toward HE by ~ 30 meV without changing the FWHM. Annealing EF *A*' reduced the FWHM from ~ 26 meV to ~ 17 meV and shifted the PL peak toward HE by ~ 41 meV. Such effects are typical of undoped MCT EFs, including those with $x \geq 0.5$ [6]. Annealing EF *B* also shifted the PL peak toward HE, whereas annealing HS *B* narrowed the PL band to an FWHM of ~ 13 meV but shifted the peak by ~ 30 meV toward LE. A similar effect occurred in structures *C* and *D*. Their PL spectra are shown in Figure 2. Their shapes are distorted by the water absorption band „φ“ ($\lambda \approx 1.38\,\mu$m).

For both the EF and HS of structure *C*, annealing shifted the PL peaks toward LE by ~ 16 meV and changed the spectral shapes (Figure 2, *a*). For structure *D*, annealing shifted the PL peaks toward LE by ~ 25 meV for the EF and ~ 45 meV for the HS, with changes in shape (Figure 2, *b*).

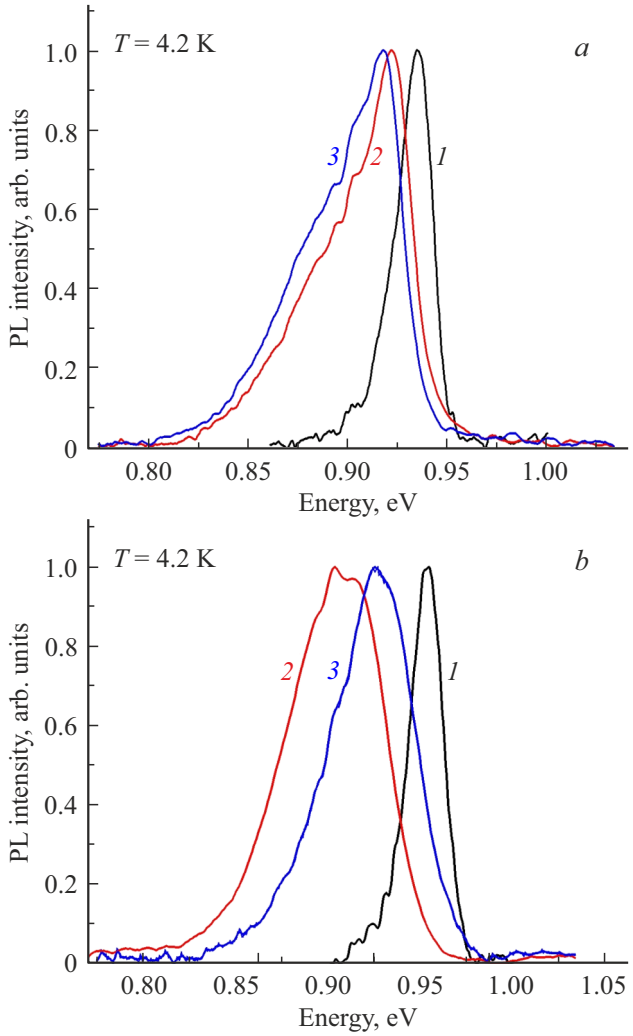


Figure 2. Normalized photoluminescence spectra of HSs *C* (*a*) and *D* (*b*) before (*1*) and after annealing (*2*); spectra *3* correspond to annealed EFs.

Table 2. EF compositions before and after annealing, determined by EDX and PL

Sample/ method	As-grown		HS annealing		EF annealing	
	EDX	PL	EDX	PL	EDX	PL
A	0.729 ± 0.001	0.730	0.736 ± 0.003	0.735	0.734 ± 0.001	0.742
A'	0.692 ± 0.002	0.696	–	–	0.714 ± 0.004	0.712
B	0.707 ± 0.001	0.712	0.709 ± 0.004	0.713	0.713 ± 0.004	0.713
C	0.718 ± 0.004	0.719	0.719 ± 0.003	0.719	0.717 ± 0.005	0.717
D	0.722 ± 0.001	0.721	0.716 ± 0.004	0.721	0.727 ± 0.004	0.726

Figure 3 shows the elemental distribution profiles in HS and EF *D* before and after annealing, obtained by EDX. Vertical dashed lines schematically indicate the heterointerfaces. Simulation of primary electron propagation using CASINO [7] for $N_e = 6000$ normally incident particles with a beam radius of $r_b = 10$ nm gave a probing length scale of ~ 600 nm. Under these conditions, the HgTe layer in the as-grown HS appeared as an increased mercury content at the surface (Figure 3, *a*). After removal of the HgTe layer, no excess surface mercury was observed, while the solid-solution component distribution remained unchanged (Figure 3, *b*).

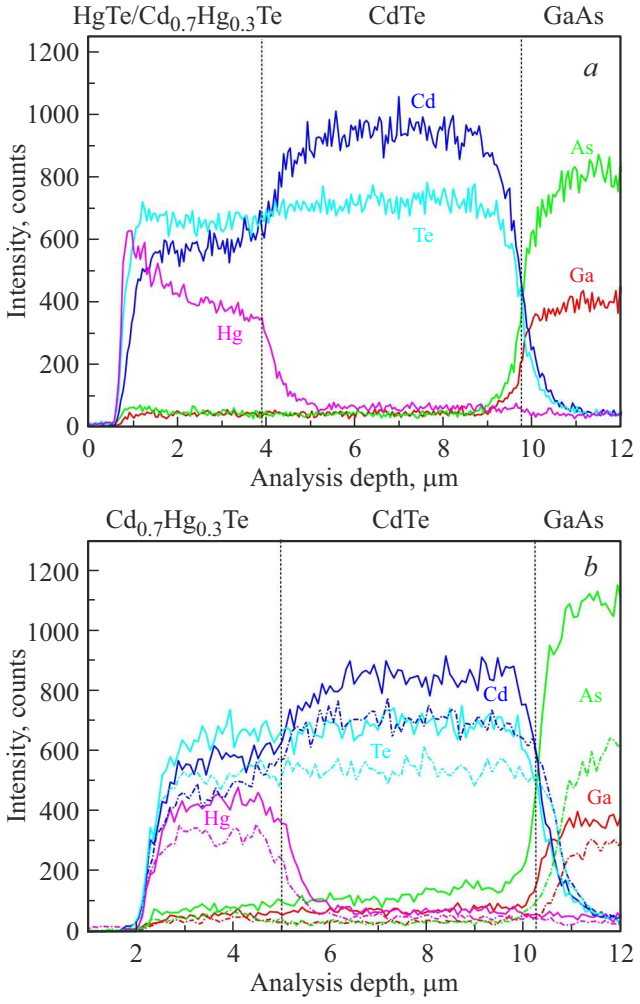


Figure 3. Elemental distribution profiles in structure *D* for the as-grown HS (*a*) and after annealing (*b*): HS followed by removal of the HgTe layer (solid lines) and EF (dash-dotted lines).

Table 2 lists the compositions x determined by EDX, averaged over three points on each sample, and by PL at $T = 293$ K (one point per sample, using the band-gap dependence $E_g(x, T)$ from Ref. [8]). For undoped MCT, annealing-induced changes, including the HE shifts of the PL peak and OT edge, are usually explained by two factors: 1) Cd diffusion from HS layers with a wider band gap than the active layer, smoothing the composition profile, as confirmed by OT and OR measurements during successive layer removal; and 2) atomic rearrangement in the lattice, reducing the magnitude of chemical composition fluctuations in the solid solution. Both effects lead to an „increase" in the average composition, as observed for structures *A* and *A'*.

As Table 2 shows, annealing doped structures with $C_{\mathrm{In}} \geq 10^{17}\,\mathrm{cm}^{-3}$ did not significantly change x. Their low-temperature PL spectra, however, changed in shape and exhibited a pronounced LE peak shift after annealing (Figure 2). The PL spectra of annealed structures *C* and *D* were analyzed assuming a narrow „band-edge" line (no broader than the original line with FWHM ~ 18 meV) and additional LE lines. This analysis suggested impurity acceptor levels with ionization energies $E_A \sim 30$ meV in both structures. These may be associated with arsenic, whose unintentional incorporation ($\sim 10^{17}\,\mathrm{cm}^{-3}$) has previously been observed in EFs grown by this process [9]. Using the approach developed in Ref. [10], E_A for arsenic in $Cd_{0.7}Hg_{0.3}Te$ is estimated at 32–37 meV.

Regarding the small composition changes accompanying pronounced LE shifts of the low-temperature PL spectra after annealing structures *B*, *C*, and *D*, indium can occupy sites in both the HgTe and CdTe sublattices of MCT [11]. We suggest that indium out-diffusion from $Cd_{0.7}Hg_{0.3}Te$ into the CdTe buffer and HgTe layer (HS annealing) or the vapor phase (EF annealing) vacates metal-sublattice sites, which are preferentially occupied by the most rapidly diffusing atoms, namely mercury. This enriches the material in mercury, producing, at high doping levels, a decrease in the average x (see Table 2 and the OT spectra in Ref. [4]). This effect can influence the optical properties of MCT not only at $T = 4.2$ K, as established here, but also at ~ 100 K [4], i. e., at the operating temperatures of many MCT devices. This highlights the relevance of the current

trend toward high-operating-temperature MCT devices [12]. In such devices, the influence of chemical composition fluctuations, an intrinsic property of solid solutions, on optical and photoelectric properties is minimized.

Thus, we investigated changes in the optical properties and chemical composition of thermally annealed indium-doped $Cd_{0.7}Hg_{0.3}Te$/HgTe heterostructures and $Cd_{0.7}Hg_{0.3}Te$ films. The results demonstrate a stabilizing effect of indium on the material properties at 300 K, but also reveal annealing-induced changes in the defect structure that can affect the optical properties at temperatures close to the operating temperatures of some CdHgTe devices.

Conflict of interest

The authors declare that they have no conflict of interest.

References

[1] A. Drago. Instruments, **9**, 12 (2025). DOI: 10.3390/instruments9020012
[2] M.A. Fadeev, A.A. Yantser, K.E. Kudryavtsev, A.A. Razova, V.V. Utochkin, V.V. Rumyantsev, A.A. Dubinov, V.Ya. Aleshkin, V.I. Gavrilenko, N.N. Mikhailov, S.V. Morozov. Appl. Optics, **65**, 177 (2026). DOI: 10.1364/AO.578783
[3] A.V. Voitsekhovskii, S.M. Dzyadukh, D.I. Gorn, N.N. Mikhailov, S.A. Dvoretsky, G.Y. Sidorov, M.V. Yakushev. J. Phys. D: Appl. Phys., **58** (3), 305101 (2025). DOI: 10.1088/1361-6463/adee2c
[4] M.S. Ruzhevich, K.D. Mynbaev, N.L. Bazhenov, M.V. Dorogov, V.S. Varavin, V.G. Remesnik, I.N. Uzhakov, N.N. Mikhailov. Fiz. Tverd. Tela, **67** (5), 805 (2025). DOI: 10.61011/FTT.2025.05.60742.131-25 (In Russian).
[5] P. Koppel. J. Appl. Phys., **57** (5), 1705 (1985). DOI: 10.1063/1.334441
[6] M.S. Ruzhevich, K.D. Mynbaev, N.L. Bazhenov, M.V. Dorogov, A.M. Smirnov, V.V. Belkov, M.V. Tomkovich, V.S. Varavin, V.G. Remesnik, I.N. Uzhakov, N.N. Mikhailov. Fiz. Tverd. Tela, **67** (1), 22 (2025). DOI: 10.61011/FTT.2025.01.59763.4-25 (In Russian).
[7] D. Drouin, A.R. Couture, D. Joly, X. Tastet, V. Aimez, R. Gauvin. Scanning, **29** (3), 92 (2007). DOI: 10.1002/sca.20000
[8] G.L. Hansen, J.L. Schmit, T.N. Casselman. J. Appl. Phys., **53** (10), 7099 (1982). DOI: 10.1063/1.330018
[9] I.I. Izhnin, A.V. Voitsekhovsky, A.G. Korotaev, O.I. Fitsych, A.Yu. Bonchyk, H.V. Savytskyy, K.D. Mynbaev, V.S. Varavin, S.A. Dvoretsky, N.N. Mikhailov, M.V. Yakushev, R. Jakiela. Infr. Phys. Technol., **81**, 52 (2017). DOI: 10.1016/j.infrared.2016.12.006
[10] K. Majkowycz, K. Murawski, M. Kopytko. Infr. Phys. Technol., **137**, 105126 (2024). DOI: 10.1016/j.infrared.2024.105126
[11] K.D. Mynbaev, V.I. Ivanov–Omskii. Fiz. Tekh. Poluprovodn., **40** (1), 3 (2006) (In Russian).
[12] A. Rogalski, M. Kopytko, F. Dai, R. Jiang, F. Wang, W. Hu, P. Martyniuk. Measurement, **230**, 114495 (2024). DOI: 10.1016/j.measurement.2024.114495